

# Cooperativity-Driven Singularities in Asymmetric Exclusion

Alan Gabel<sup>1</sup> and S. Redner<sup>1</sup>

<sup>1</sup>Center for Polymer Studies and Department of Physics, Boston University, Boston, Massachusetts 02215, USA

E-mail: agabel@bu.edu, redner@bu.edu

**Abstract.** We investigate the effect of cooperative interactions on the asymmetric exclusion process, which causes the particle velocity to be an increasing function of the density. Within a hydrodynamic theory, initial density upsteps and downsteps can evolve into: (a) shock waves, (b) continuous compression or rarefaction waves, or (c) a mixture of shocks and continuous waves. These unusual phenomena arise because of an inflection point in the current versus density relation. This anomaly leads to a group velocity that can either be an increasing or a decreasing function of the density on either side of the inflection point, a property that underlies these localized wave singularities.

PACS numbers: 02.50.-r, 05.40.-a

## 1. Introduction

The asymmetric exclusion process (ASEP) [1, 2, 3, 4, 5] represents an idealized description of transport in crowded one-dimensional systems, such as traffic [6, 7, 8], ionic conductors [9], and RNA transcription [10]. In the ASEP, each site is either vacant or occupied by a single particle that can hop at a fixed rate to a vacant right neighbor [1, 2, 3, 4]. Although simply defined, this model has rich transport properties: for example, density heterogeneities can evolve into rarefaction or shock waves [4], while an open system, with input at one end and output at the other, exhibits a variety of phases as a function of the input/output rates [11, 12, 13].



**Figure 1.** Cooperative exclusion. A “pushed” particle — one whose left neighbor is occupied — can hop to a vacant right neighbor with rate 1, while an isolated particle hops to a vacancy with rate  $\lambda$ .

A fundamental property of the ASEP is the relation  $J(\rho) = \rho(1 - \rho)$  between the current  $J$  and density  $\rho$ . Because each site is occupied by at most one particle, the average particle velocity  $v = J/\rho$  is a decreasing function of the density. In this work, we investigate a *cooperative exclusion* (CE) model in which the velocity can *increase* with density. This cooperativity leads to unexpected features in the evolution of initial density heterogeneities. Such cooperativity occurs, for example, when ants emit pheromones that help guide fellow ants along a trail [14]. Another example are multiple buses that follow a fixed route. The leading bus picks up more passengers so that the next bus moves faster, which causes clustering of buses during peak travel times [15]. At the microscopic level, molecular motors can work together to pull a load that is too large for a single motor [16]. Cooperativity has even been proposed as a basis for organic superconductors [17].

## 2. Cooperative Exclusion Model

In the CE model, a particle can hop to its vacant right neighbor at a rate  $r$  that depends on the occupancy of the previous site (Fig. 1):

$$r = \begin{cases} 1 & \text{previous site occupied,} \\ \lambda & \text{previous site vacant,} \end{cases}$$

with  $0 \leq \lambda \leq 1$ . When  $\lambda = 1$ , the standard ASEP is recovered, while  $\lambda = 0$  corresponds to *facilitated* asymmetric exclusion [18], in which the left neighbor of a particle must be occupied for the particle to hop to a vacancy on the right. We pictorially view this restriction as a particle requires a “push” from its left neighbor to hop. This facilitation causes an unexpected discontinuity in a rarefaction wave in the ASEP [19].

More strikingly, we will show that cooperativity leads to shock and rarefaction waves that can be continuous, discontinuous, or a mixture of the two.

These unusual features arise in CE when  $0 < \lambda < \frac{1}{2}$ , where an inflection point in  $J(\rho)$  occurs at  $\rho = \rho_I$  (Fig. 2). For  $\rho < \rho_I$ , cooperativity dominates, and  $J$  grows superlinearly in  $\rho$ . At higher densities, excluded volume interactions dominate, so that  $J$  grows sublinearly and ultimately decreases to zero. Correspondingly, the group velocity changes from an increasing to a decreasing function of density  $\rho$  as  $\rho$  passes through  $\rho_I$ .

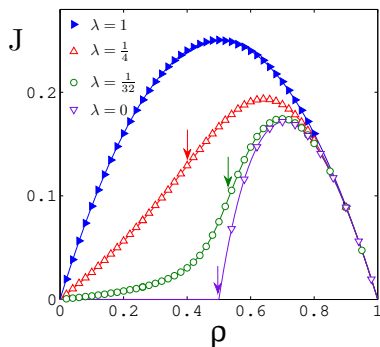


**Figure 2.** Steady state current as function of density in cooperative exclusion (CE). Data are based  $10^2$  realizations with  $L = 10^3$  up to  $t = 10^4$ . The solid curves are given by Eq. (3). Arrows indicate the locations of the inflection points.

A configuration of  $N$  particles on a ring of length  $L$  is specified by the occupation numbers  $\{n_1, \dots, n_L\}$ , subject to conservation  $\sum_i n_i = N$ ; here  $n_i$  equals 1 if  $i$  is occupied and equals 0 otherwise. A crucial feature of CE is that the probability for any steady-state configuration is a *decreasing* function of the number  $k$  of adjacent vacancies:  $k \equiv \sum_{i=1}^L (1 - n_i)(1 - n_{i+1})$ , with  $n_{L+1} = n_1$ . To understand how the configurational probabilities depend on  $k$ , we observe that the hopping of a pushed particle (whose left neighbor is occupied) either preserves or decreases the number of adjacent vacancies  $k$  (Fig. 3(a),(b)). Conversely, the hopping of an isolated particle either preserves or increases  $k$ . Since pushed particle hopping events occur at a higher rate, configurations with fewer adjacent vacancies are statistically more probable.

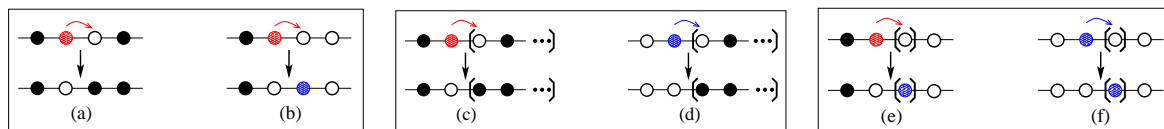


**Figure 3.** [left] Hopping of a pushed particle where the number of vacancies is (a) preserved or (b) decreases. [middle] Creation of a cluster of length  $\geq 2$  in  $\mathcal{C}$  (demarcated), by the (c) hopping of a pushed particle or (d) an isolated particle. [right] Creation of a cluster of length 1 (demarcated) in  $\mathcal{C}$  by (e) hopping of a pushed particle or (f) an isolated particle.

We argue that the probability  $P_k$  for a configuration with  $k$  adjacent vacancies is

$$P_k = \frac{\lambda^k}{Z(\lambda)}, \quad (1)$$

where  $Z(\lambda)$  is a normalization constant. To justify (1), we show that it satisfies the detailed balance condition in the steady state, for which the overall rate of entering and leaving a configuration  $\mathcal{C}$  must be equal:

$$P(\mathcal{C}) \sum_{\mathcal{C}'} R(\mathcal{C} \rightarrow \mathcal{C}') = \sum_{\mathcal{C}'} P(\mathcal{C}') R(\mathcal{C}' \rightarrow \mathcal{C}). \quad (2)$$

Here  $P(\mathcal{C})$  is the probability of configuration  $\mathcal{C}$  and  $R(\mathcal{C} \rightarrow \mathcal{C}')$  is the transition rate from  $\mathcal{C}$  to  $\mathcal{C}'$ . The left side corresponds to all ways of exiting  $\mathcal{C}$ , while the right side corresponds to ways of entering  $\mathcal{C}$ .

Evolution out of a configuration occurs when the front particle in any cluster hops. There are two contributing processes: either a particle is pushed at rate 1 from a cluster of length  $\geq 2$ , or an isolated particle hops at rate  $\lambda$ . Thus  $\sum_{\mathcal{C}'} R(\mathcal{C} \rightarrow \mathcal{C}') = G_2 + \lambda c_1$ , where  $G_2$  is the number of clusters of length  $\geq 2$  and  $c_1$  is the number of unit-length clusters in  $\mathcal{C}$ . To compute the right side of Eq. (2), we enumerate all events that lead into  $\mathcal{C}$ . Each involves the hopping of a particle to become the end of a cluster in  $\mathcal{C}$ . There are two contributing processes: a cluster of length  $\geq 2$  is created when either a pushed particle or an isolated hops to the trailing end of a cluster of length  $\geq 1$  (Fig. 3(c),(d)). For a pushed particle, the hopping rate is 1 and the relative weights of the initial and final configurations are equal because the number of vacancy pairs  $k$  is unchanged. For an isolated particle, the hopping rate is  $\lambda$ , but the initial configuration has a relative weight  $\frac{1}{\lambda}$ , by Eq. (1), because the hop increases the number of vacancy pairs by 1. Since these processes occur for every cluster of size  $\geq 2$ , their total weight is  $G_2$ .

Similarly, a unit-length cluster is created by the hopping of a pushed or an isolated particle. A pushed particle (Fig. 3(e)) hops with rate 1 from a configuration with relative weight  $\lambda$  compared to the final state (since  $k$  decreases by 1), while an isolated particle (Fig. 3(f)) hops with rate  $\lambda$  from a configuration with relative weight 1 (since  $k$  is unchanged). The total weight of these processes is  $\lambda c_1$ . Thus the sum of the weights of the entrance processes to configuration  $\mathcal{C}$  balances those of the exit processes when each configuration has weight proportional to  $\lambda^k$ .

We now exploit the work of Antal and Shütz [7] who investigated a dual model in which next-nearest neighbor cooperative interactions pull a particle ahead, in contrast to our pushing particles from behind. By mapping particles  $\leftrightarrow$  holes, it is clear that both models have the same probability distribution and steady-state current [7]

$$J = (1 - \rho) \left[ 1 + \frac{\sqrt{1 - 4(1 - \lambda)\rho(1 - \rho)} - 1}{2(1 - \lambda)\rho} \right] \quad (3)$$

in the  $L \rightarrow \infty$  limit. The salient feature is that  $J$  has an inflection point at a density  $\rho_I$  for  $\lambda < \frac{1}{2}$  (Fig. 2). We henceforth restrict our analysis to this domain.

### 3. Density Profile Dynamics

In a hydrodynamic description, the particle satisfies the continuity equation  $\rho_t + J_x = 0$ . By the chain rule, we rewrite the second term as  $J_\rho \rho_x$ , from which the group velocity  $u = J_\rho$ . Here the subscripts  $t, x, \rho$  denote partial differentiation. The crucial feature is the inflection point in  $J(\rho)$ , so that the group velocity can be either increasing or decreasing in  $\rho$ . We now employ the steady-state current (3) to determine the evolution of an initial density heterogeneity on length and time scales large compared to microscopic scales for the step initial condition

$$\rho(x, t = 0) = \begin{cases} \rho_- & x \leq 0, \\ \rho_+ & x > 0. \end{cases} \quad (4)$$

As sketched in Fig. 4, the difference in the group velocity to the right and left of the step determines whether a continuous, discontinuous, or a composite density profile emerges.

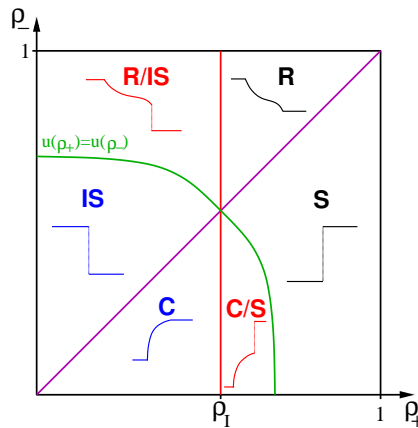


**Figure 4.** Phase diagram of the CE model for an initial density step  $(\rho_-, \rho_+)$ , with  $\rho_I$  the inflection point in  $J(\rho)$ . A typical density profile  $\rho(z)$  is sketched for each of the six regions: (R/IS) rarefaction/inverted shock, (R) continuous rarefaction, (S) shock, (C/S) compression/shock, (C) continuous compression, (IS) inverted shock.

*Shock/Inverted Shock:* A propagating shock wave arises whenever the group velocity on the left exceeds that on the right,  $u(\rho_-) > u(\rho_+)$ . Qualitatively, the faster moving particles catch up to slower particles on the right and pile up in a shock wave, just as freely-moving cars suddenly slow down upon approaching a traffic jam. In the conventional ASEP, all upsteps evolve into a *shock* (S) wave. For the CE, in contrast, only upsteps where both initial densities are above the inflection point,  $\rho_I < \rho_- < \rho_+$ , evolve into shocks (Fig. 5). Here, exclusion is sufficiently strong that the group velocity is a decreasing function of density. Strikingly, a propagating shock wave also emerges from a downstep in CE when the initial densities are both below the inflection point,  $\rho_I > \rho_- > \rho_+$ . In this regime,  $J_{\rho\rho} = u_\rho > 0$ ; that is, cooperativity is sufficiently strong that particles in the high-density region on the left have a greater group velocity

and therefore pile up at the interface. We term this singularity an *inverted shock* (IS) (Fig. 5).

For both shocks and inverted shocks, the density is given by the traveling wave profile  $\rho = \rho(x - ct)$ . We obtain the shock speed  $c$  by equating the net flux into a large region that includes the shock,  $J(\rho_+) - J(\rho_-)$ , with the change in the number of particles,  $c(\rho_+ - \rho_-)$ , in this region [20] to obtain the standard expression  $c = [J(\rho_+) - J(\rho_-)]/[\rho_+ - \rho_-]$ ; this holds both for conventional and inverted shocks.

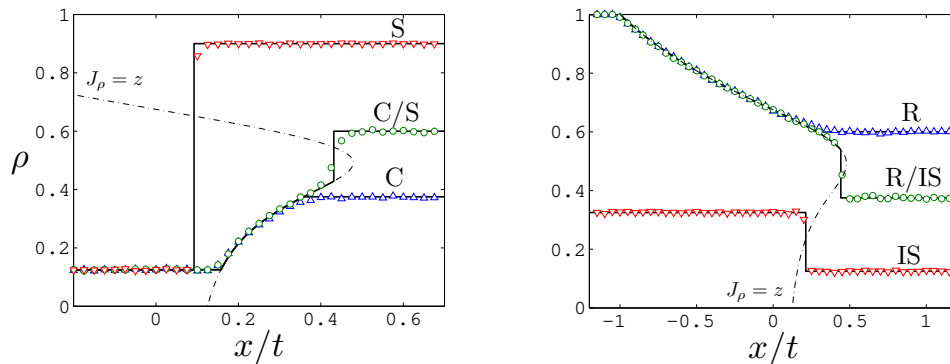


**Figure 5.** (left) Evolution of an upstep for  $\lambda = \frac{1}{8}$ : (C) continuous compression wave for  $\rho_- = \frac{1}{8}$ ,  $\rho_+ = \frac{3}{8}$ ; (C/S) composite compression/shock for  $\rho_- = \frac{1}{8}$ ,  $\rho_+ = \frac{6}{10}$ ; (S) shock for  $\rho_- = \frac{1}{8}$ ,  $\rho_+ = \frac{9}{10}$ . (right) Evolution of a downstep for  $\lambda = \frac{1}{8}$ : (R) continuous rarefaction for  $\rho_- = 1$ ,  $\rho_+ = \frac{6}{10}$ ; (R/IS) composite rarefaction/inverted shock for  $\rho_- = 1$ ,  $\rho_+ = \frac{3}{8}$ ; (IS) inverted shock for  $\rho_- = 0.325$ ,  $\rho_+ = \frac{1}{8}$ . The dashed line is the locus  $J_\rho = z$  and the solid black curves are analytic predictions. Simulations are based on  $10^3$  realizations up to  $t = 4 \times 10^3$ .

*Continuous Rarefaction/Compression:* A density step gradually smooths out when the when the group velocity to the left is less than that on the right,  $u(\rho_-) < u(\rho_+)$ . Here the faster particles on the right leave open space for the slower particles, similar to a cluster of stopped cars that slowly spreads out after a stoplight turns green. In ASEP, a downstep always evolves to a *continuous rarefaction* (R) wave. This continuous rarefaction also occurs in CE when both initial densities are above the inflection point,  $\rho_- > \rho_+ > \rho_I$ . At these high densities, exclusion dominates, as in the ASEP, which causes the group velocity to decrease with density.

In striking contrast to the ASEP, an upstep can continuously smooth out in CE when the initial densities are below the inflection point,  $\rho_- < \rho_+ < \rho_I$ . In this regime, cooperativity is sufficiently strong that particles in the high density region on the right move faster than those on the left. Thus instead of a shock wave, a *continuous compression* (C) wave develops (Fig. 5). We determine the density profile by assuming that it is a function of the scaled variable  $z = x/t$ . Substituting  $\rho(x, t) = \rho(z)$  into the continuity equation gives  $-z\rho_z + J_\rho \rho_z = 0$ . Thus the profile consists either of constant-

density segments ( $\rho_z = 0$ ) or else  $z = J_\rho$ . Matching these solutions gives [5, 19]

$$\rho(z) = \begin{cases} \rho_- & z < z_- , \\ I(z) & z_- \leq z \leq z_+ , \\ \rho_+ & z > z_+ , \end{cases} \quad (5)$$

where  $I(z)$  is the inverse function of  $z = J_\rho$ . For a continuous profile, the cutoffs  $z_-$  and  $z_+$  are determined by matching the interior solution  $I(z)$  with the asymptotic solutions:  $I(z_\pm) = \rho_\pm$  or equivalently,  $z_\pm = J_\rho(\rho_\pm)$ .

*Composite Rarefaction/Compression and Shock:* In CE, a continuous rarefaction or compression wave can coexist with a shock wave. This phenomenon occurs when the group velocity on the left is initially less than that on the right but also with the constraint that the initial densities lie on either side of the inflection point. Consequently one side of the step is in the exclusion-dominated regime and the other is in the cooperativity-dominated regime, or vice-versa. In particular, a *composite rarefaction/inverted shock* (R/IS) wave emerges from a downstep when  $\rho_- > \rho_I > \rho_+$ , so that  $u(\rho_-) < u(\rho_+)$ . As in the case of the continuous rarefaction wave, the downstep begins to smooth out from the rear. Consequently, cooperative interactions become more important as the density at the leading edge of this rarefaction decreases. Eventually this leading density reaches the point where the particle speed matches that at the bottom of the downstep and the rarefaction front terminates in an inverted shock.

Correspondingly, an upstep can evolve to a compression wave with a leading shock when the densities satisfy  $\rho_- < \rho_I < \rho_+$  and  $u(\rho_-) < u(\rho_+)$ . In this case, the leading particles initially race ahead, leaving behind a profile where the density increases with  $x$ . However, this increase cannot be continuous because eventually a point is reached where the speed at the front of this continuous wave matches that of the top of the upstep. After this point, a pile-up occurs and a shock wave forms. We call this profile a *composite compression/shock* (C/S) wave (Fig. 5).

The functional forms of the composite rarefaction/inverted shock and composite compression/shock profiles are still given by Eq. (5), but the criteria to determine the cutoffs  $z_\pm$  are now slightly more involved than for continuous profiles. The location of the left cutoff,  $z_-$ , is again determined by continuity, namely,  $I(z_-) = \rho_-$  or, alternatively,  $z_- = J_\rho(\rho_-)$ . To determine the right cutoff  $z_+$ , note that in a small spatial region that includes the leading-edge discontinuity, the density profile is just that of a shock or inverted shock wave. Thus the equation for the shock speed is

$$z_+ = \frac{J(q_+) - J(\rho_+)}{q_+ - \rho_+} , \quad (6)$$

where  $q_+ \equiv I(z_+)$  is the density just to the left of the discontinuity. (Note also that  $z_+ = J_\rho(q_+)$  by definition.) To justify (6), we use the conservation equation that the particle number in  $[z_-, z_+]$  equals the initial number plus the net flux into this region:

$$\int_{z_-}^{z_+} I(z) dz = -\rho_- z_- + \rho_+ z_+ - J(\rho_+) + J(\rho_-) . \quad (7)$$

We recast this expression into (6), by making the variable change  $z = J_\rho(\rho)$  and using  $I(J_\rho(\rho)) = \rho$  to write the integral as  $\int_{\rho_-}^{q+} \rho J_{\rho\rho} d\rho$ , which can be performed by parts. The resulting expression readily simplifies to (6).

In summary, a diversity of wave singularities arise in asymmetric exclusion with sufficiently strong cooperativity. The minimum requirement for these phenomena is an inflection point in the current-density relation  $J(\rho)$ . This inflection point leads to a group velocity that is an *increasing* function of density for  $\rho < \rho_I$ , a dependence opposite to that in the conventional ASEP. The resulting non-monotonic density dependence of the velocity causes an initial density upstep or downstep to evolve to: shock/inverted shocks, continuous rarefaction/compression waves, or a composite profile with both continuous and discontinuous elements.

## Acknowledgments

We thank Martin Schmalz for asking an oral exam question that helped spark this work and Paul Krapivsky for helpful discussions. We also gratefully acknowledge financial support from NSF grant DMR-0906504.

## References

- [1] B. Schmittmann and R. K. P. Zia, in *Phase Transitions and Critical Phenomena*, Vol. 17, eds. C. Domb and J. L. Lebowitz (Academic Press, London, 1995).
- [2] B. Derrida, Phys. Repts. **301**, 65 (1998); J. Stat. Mech. P07023 (2007).
- [3] G. Schütz, in *Phase Transitions and Critical Phenomena*, Vol. 19, eds. C. Domb and J. L. Lebowitz (Academic Press, London, 2000).
- [4] R. A. Blythe and M. R. Evans, J. Phys. A **40**, R333 (2007).
- [5] P. L. Krapivsky, S. Redner, and E. Ben-Naim, *A Kinetic View of Statistical Physics* (Cambridge University Press, Cambridge, 2010).
- [6] V. Popkov and G. M. Schütz, Europhys. Lett. **48**, 257 (1999).
- [7] T. Antal and G. M. Schütz, Phys. Rev. E **62**, 83 (2000).
- [8] A. Schadschneider, D. Chowdhury, and K. Nishinari, *Stochastic Transport in Complex Systems: From Molecules to Vehicles*, (Elsevier, 2010).
- [9] P. M. Richards, Phys. Rev. B **16**, 1393 (1977).
- [10] C. T. MacDonald, J. H. Gibbs, and A. C. Pipkin, Biopolymers **6**, 1 (1968); C. T. MacDonald and J. H. Gibbs, Biopolymers **7**, 707 (1969).
- [11] J. Krug, Phys. Rev. Lett. **67**, 1882 (1991).
- [12] B. Derrida, E. Domany, and D. Mukamel, J. Stat. Phys. **69**, 667 (1992).
- [13] G. M. Schütz and E. Domany, J. Stat. Phys. **72**, 277 (1993).
- [14] M. Burd, D. Archer, N. Aranwela, and D. J. Stradling, Am. Nat. **159**, 283 (2002).
- [15] O. J. O’Loan, M. R. Evans, and M. E. Cates, Phys. Rev. E **58**, 1404 (1998).
- [16] D. Chowdhury, Physica A **372**, 84 (2006).
- [17] W. A. Little, Phys. Rev. Lett. **134**, A1416 (1964); Sci. Am. **212**, 21 (1965).
- [18] U. Basu and P. K. Mohanty, Phys. Rev. E **79**, 041143 (2009).
- [19] A. Gabel, P. L. Krapivsky, and S. Redner, Phys. Rev. Lett. **105**, 210603 (2010).
- [20] G. B. Whitham, *Linear and Nonlinear Waves* (Wiley, New York, 1974).